Synthesis, Structure, Optical Properties, and Magnetism of the Manganese Chalcogenide Beryllosilicate and Beryllogermanate Sodalites

S. E. Dann,[†] M. T. Weller,*[,†] B. D. Rainford,[‡] and D. T. Adroja[‡]

Departments of Chemistry and Physics, University of Southampton, Highfield, Southampton SO17 1BJ, U.K.

Received May 1, 1997[⊗]

The compounds $Mn_8[BeSiO_4]_6X_2$ (X = S, Se, Te) $Mn_8[BeGeO_4]_6X_2$ (X = S, Se) have been synthesized by solid state reactions of the constituent oxides and MnX at 1000−1100 °C in sealed quartz ampules. The materials crystallize with the cubic sodalite unit cell with an ordered Be/Z^{4+} (Z^{4+} = Ge/Si) framework in the space group $P\bar{4}3n$. Their structures have been refined from powder X-ray and/or powder neutron diffraction data in order to investigate the coordination geometry of the encapsulated Mn_4X unit. The energies of the d−d transitions in the UV/vis spectra are characteristic of high-spin d^5 tetrahedral manganese. Correlations between structural parameters and IR absorptions are reported for the families of beryllosilicate and beryllogermanate frameworks $M_8[BeZO_4]_6X_2$ (M = Cd, Mn; Zn, Z = Si, Ge; X = S, Se, Te). Preliminary magnetic measurements on the manganese-containing compounds indicate strong antiferromagnetic interactions, of order 100 K, between Mn^{2+} ions, but the observation of rounded maxima in the susceptibility at 10 K suggests spin-glass freezing rather than long-range magnetic order, indicating a high degree of geometrical frustration between the tetrahedrally coordinated spins of the Mn_4X cluster.

Introduction

The sodalites form a diverse class of anion-containing frameworks consisting of β-cages formed from (Be, Al, Ga, Si, Ge, Zn, or P)O_4 tetrahedra; centrally placed in the β-cage is an anion tetrahedrally coordinated to four cations. The coordination of each cation is more complex with three strong and three weak interactions with the oxygens in the β-cage six-ring and one strong interaction with the central anion.[1] In extreme cases, where the cation is small, the coordination is essentially tetrahedral where the three weak interactions with the oxygen in the six-ring become nonbonding.

The aluminosilicates are the most well studied group of sodalite materials, with general formula $M_8[AlSiO_4]_6X_n$, and have been shown to incorporate a wide range of cations, anions, and neutral species including Cl, Br, I, SCN, NO_2, SO_4, MnO_4, CrO_4, ClO_4, S, CO_3, $B(OH)_4$, 1,3-dioxolane.[2−5] Of note, as members of this class, are the well-known ultramarines which contain the polysulfide and polyselenide anion radicals and are widely used as pigments.

Recently the sodalites consisting of a framework solely made up of AlO_4 tetrahedra, with general formula $M_8[AlO_2]_{12}X_2$, have attracted much interest. These materials are unusual in that they disobey Löwenstein's rule of aluminum avoidance but are still readily synthesized at high temperature.[6−8] In these materials, the extraframework ions are divalent and tend to be larger due to the increase in size of the framework. Related are the borate sodalites $M_8[BO_2]_{12}X_2$ which have smaller cages suitable for coordinating to smaller divalent cations such as zinc and cobalt.[9]

Framework structures containing the more uncommon TO_4 tetrahedra have been less well studied. Recent interest in the area has produced novel materials such as the berylloarsenates,[10] silica sodalite,[11] or the aluminogermanates.[12] Even more unusual is the phosphonitride sodalite framework of $Zn_7[P_{12}N_{14}]Cl_2$ synthesized and investigated by Schnick.[13] The beryllogermanate/beryllosilicate sodalites are compositionally equivalent to the aluminate sodalites but have remained poorly investigated despite the occurrence of the beryllosilicate minerals genthelvite, helvite, and danalite[14,15] in nature. Recently work initiated by Mel'nikov[16] was continued on materials of this type by carrying out structural investigations on the series $Cd_8[BeZO_4]_6X_2$ (Z = Si, Ge; X = S, Se, Te), where previously only lattice constants had been reported.[17,18] These materials are analogous to $Cd_8[AlO_2]X_2$ (X = S, Se) and $Zn[BO_2]X_2$ (X = O, S, Se),[19−21] where the sodalite cage may be considered to contain small blocks of (II,VI) semiconductor. Electronic interaction between these units would be of considerable interest as these materials could be considered to be framework-expanded semiconductors.

[†] Department of Chemistry.
[‡] Department of Physics.
[⊗] Abstract published in *Advance ACS Abstracts,* October 15, 1997.

(1) Pauling, L. *Z. Kristallogr.* **1930,** 74, 213.
(2) Barrer, R. M.; Cole, R. F.; Villiger, H. *J. Chem. Soc. A* **1970**, 1524.
(3) Hund, F. *Z. Anorg. Allg. Chem.* **1984** *511,* 255.
(4) Haworth, K.; Weller, M. T. *J. Chem. Soc., Chem. Commun*. **1991**, *10,* 734.
(5) van de Goor, G.; Behrens, P.; Felsche J. *Microporous Mater*. **1994**, *2,* 493.
(6) Kondo, R. *Yogyo Kyokaishi* **1965**, *71,* 1.
(7) Brenchley, M. E.; Weller, M. T. *J. Mater. Chem*. **1992**, *2,* 1003.
(8) Dann, S. E.; Weller, M. T. *J. Mater. Chem*. **1996**, *6,* 1717.
(9) Fouassier, C.; Levasseur, A.; Joubert J. C.; Muller J.; Hagenmuller P. *Z. Anorg. Allg. Chem*. **1970**, *375,* 202.
(10) Harrison, W. T. A.; Gier, T. E.; Stucky, G. D. *Acta Crystallogr*. **1994**, *C50,* 471.
(11) Bibby, D. M.; Dale, M. P. *Nature* **1985**, *317,* 157.
(12) Fleet, M. E. *Acta Crystallogr*. **1989**, *C45*, 843.
(13) Schnick, W.; Lücke, J. *Z. Anorg. Allg. Chem*. **1994**, *620,* 2014.
(14) Hassan, I.; Grundy, H. D. *Am. Mineral*. **1985**, *70,* 186.
(15) Holloway, W. M.; Giordano, T. J.; Peacor, D. R. *Acta Crystallogr*. **1972**, *B28*, 114.
(16) Mel'nikov, O. K.; Latvin, B. M.; Fedosova, S. P. In *Gidrotermal'nyi Sintez Kristallov*; Lobacher, A.M., Ed.; Nauka Press: Moscow, 1968; p 167.
(17) Dann, S. E.; Weller, M. T. *Inorg. Chem.* **1996**, *35*, 555.
(18) Dann, S. E.; Weller, M. T. *Prog. Zeolite Microporous Mater*. **1997**, *105*, 2131.
(19) Smith-Verier, P.; Garcià-Blanco, S. *Z. Kristallogr.* **1980**, *151*, 175.
(20) Brenchley, M. E.; Weller, M. T. *Angew. Chem., Int. Ed. Engl.* **1993**, *32*, 1663.
(21) Brenchley, M. E. Ph.D. Thesis, University of Southampton, 1994; p 99.

S0020-1669(97)00511-9 CCC: $14.00

The electronic properties of $Zn_8[BO_2]_{12}X_2$[22] and $Zn_8[BeSiO_4]_6X_2$[23] (X = S, Se, Te) and $Ga_xZn_{8-x}P_x[BO_2]_{12}Se_{2-x}$[24] were investigated by Moran *et al.* This work describes the optical absorption bands as having a large blue shift away from those of the bulk MX materials; rather than describing this as a blue-shifted absorption, the optical spectrum could be described as that expected for discrete M_4X units. The electrostatic isolation effect of the framework was also demonstrated in the ^{77}Se and ^{125}Te MAS NMR spectra, which exhibited upfield shifts from the resonances of the bulk MX materials. This indicated a reduction in the paramagnetic contribution to the chemical shift, suggesting greater localization of the electron density in the sodalite compared with that of the bulk MX. These authors also mention the synthesis of the cadmium-containing beryllosilicates and beryllogermanates,[23] but little structural information was presented. Recent investigations on the structural and electronic properties of $Cd_8[BeSiO_4]_6X_2$[17] and $Cd_8[BeGeO_4]_6X_2$[18] have shown that, despite the shortest relative M−X intercage separation in relation to the bulk M−X bond distance in CdTe beryllosilicate sodalite compared with other members of the sodalite family, the M−X distance is still 50% greater than for the bulk M−X material and there is no appreciable electronic interaction. Similar results were also noted for the material $Cd_8[AlO_2]_{12}S_2$,[20] whose optical properties showed a large blue shift of the absorption edge associated with the electronic isolation of the CdS units by the framework and a smaller blue-shifted edge due to small amounts of bulk CdS on the surface of the sodalite.[25]

The manganese sulfide beryllosilicate and beryllogermanate sodalites were also prepared by Mel'nikov *et al.*,[16] but no structural characterization was performed. Although synthesis of the selenide and telluride analogues was attempted in this study, the high-pressure hydrothermal route was unsuccessful. An additional feature of these manganese sodalites is the presence of the Mn^{2+} magnetic centers; the distribution of these centers as discrete tetrahedral Mn_4X units separated by approximately 5 Å presents an unusual array with the potential for both local and long-range interactions.

In this paper, we report synthesis of the manganese beryllosilicates and beryllogermanates, their structure, and characterization of their spectroscopic/magnetic properties.

Results and Discussion

X-ray Refinement/Neutron Refinement. Refinement was carried out in the space group $P\bar{4}3n$ using the starting model of helvite[15] with an ordered framework consisting of alternating BeO_4 and ZO_4 tetrahedra (Z = Si/Ge). The program GSAS[26,27] was used for the refinement. Initial stages of the refinement of the $Mn_8[BeZO_4]_6X_2$ phases included all instrument parameters; atomic parameters were slowly introduced, and in the latter stages all atomic positional parameters were varied. Final stages of the neutron refinement included isotropic temperature factors for all atoms, but in the X-ray refinement the beryllium temperature factor was set at unity due to its nominal X-ray scattering. Final atomic parameters are summarized in Table 1, and important bond angles are given in Table 2. Structures refined from powder X-ray data are identified in Table 1. An example of the profile fit achieved is given in Figure 1. EDAX analysis on individual crystals and larger areas consisting of many particles showed the Mn:Z:X ratio to approximate to 4:3:1, in good agreement with the targeted stoichiometry in all cases. The crystallites formed as polyhedra with rounded terminations and particle sizes between 5 and 20 μm. The crystallites were uniform in appearance, and no evidence for additional phases of differing morphologies was seen.

Table 1. Refined Atomic Parameters (Esd's Given in Parentheses)

atom	site	*x*	*y*	*z*	*B* (Å^2)
		(a) $Mn_8[BeSiO_4]_6S_2$			
Be	6c	0.25	1/2	0	0.56(7)
Si	6b	0.25	0	1/2	0.60(11)
Mn	8c	0.1706(3)	0.1706(3)	0.1706(3)	0.47(8)
O	24i	0.1392(4)	0.1421(5)	0.4172(2)	0.71(10)
S	2a	0	0	0	0.70(18)
		a = 8.3005(1) Å; R_{wp} = 5.75%; χ^2 = 15.51			
		(b) $Mn_8[BeSiO_4]_6Se_2$[a]			
Be	6c	0.25	1/2	0	1.00
Si	6b	0.25	0	1/2	2.92(48)
Mn	8c	0.1782(5)	0.1782(5)	0.1782(5)	2.16(23)
O	24i	0.1407(5)	0.1396(10)	0.4185(7)	1.84(51)
Se	2a	0	0	0	2.21(30)
		a = 8.3310(3) Å; R_{wp} = 5.72%; χ^2 = 11.25			
		(c) $Mn_8[BeSiO_4]_6Te_2$[a]			
Be	6c	0.25	1/2	0	1.00
Si	6b	0.25	0	1/2	2.05(31)
Mn	8c	0.1879(4)	0.1879(4)	0.1879(4)	2.56(20)
O	24i	0.1443(12)	0.1444(12)	0.4270(9)	1.45(31)
Te	2a	0	0	0	2.12(13)
		a = 8.4262(4) Å; R_{wp} = 6.70%; χ^2 = 11.29			
		(d) $Mn_8[BeGeO_4]_6S_2$			
Be	6c	0.25	1/2	0	0.26(7)
Ge	6b	0.25	0	1/2	0.81(9)
Mn	8c	0.1672(3)	0.1672(3)	0.1672(3)	0.75(6)
O	24i	0.1452(3)	0.1356(3)	0.4088(2)	0.82(12)
S	2a	0	0	0	1.06(14)
		a = 8.4549 (1) Å; R_{wp} = 3.91%; χ^2 = 3.72			
		(e) $Mn_8[BeGeO_4]Se_2$			
Be	6c	0.25	1/2	0	2.92(17)
Ge	6b	0.25	0	1/2	1.44(15)
Mn	8c	0.1737(6)	0.1737(6)	0.1737(6)	2.54(21)
O	24i	0.1402(10)	0.1425(10)	0.4116(4)	2.28(8)
Se	2a	0	0	0	2.12(15)
		a = 8.5153(3) Å; R_{wp} = 12.01%; χ^2 = 3.83			

[a] Structures were refined from powder X-ray data.

Table 2. Derived Bond Distances (Å) and Angles(deg) for $Mn_8[BeZO_4]_6X_2$ (Esd's Given in Parentheses)

atoms	Z = Si, X = S	Z = Si, X = Se	Z = Si, X = Te	Z = Ge, X = S	Z = Ge, X = Se
Be−O1	1.616(4)	1.625(3)	1.629(9)	1.642(3)	1.682(11)
Z−O1	1.646(4)	1.637(3)	1.627(9)	1.742(3)	1.707(11)
Mn−O1	2.076(3)	2.052(6)	2.080(11)	2.069(3)	2.063(5)
Mn−X	2.453(5)	2.571(7)	2.743(6)	2.449(4)	2.562(9)
Be−O−Si	128.24(13)	129.06(33)	132.04(7)	124.07(10)	125.36(20)

Vibrational Spectra. The vibrational spectra of sodalites are characteristic of the framework geometry and have been investigated by a number of groups.[28−30] Creighton *et al.*[29] fully

(22) Moran, K. L.; Harrison, W. T. A.; Gier, T. E.; MacDougall, J. E.; Stucky, G. D. *Mater. Res. Soc. Symp. Proc.* **1990**, *164*, 123.
(23) Moran, K. L.; Harrison, W. T. A.; Gier, T. E.; Eckert, H.; Ott W.; Stucky G. D. *Mater. Res. Soc. Symp. Proc.* **1992**, *242*, 249.
(24) Moran, K. L.; Harrison, W. T. A.; Gier, T. E.; Eckert, H.; Eichele, K.; Wasylishen, R. E.; Stucky, G. D. *J. Am. Chem. Soc.* **1993**, *115*, 10553.
(25) Blasse, G.; Dirken, G. J.; Brenchley, M. E.; Weller, M. T. *Chem. Phys. Lett.* **1995**, *234*, 177.
(26) Larson, A. C.; von Dreele, R. B. *GSAS: Generalised Structural Analysis System;* Los Alamos National Laboratory: Los Alamos, NM, 1990.
(27) Henderson, C. M. B.; Taylor, D. *Spectrochim. Acta* **1977**, *33A*, 283.
(28) Taylor, M. J.; Marshall, D. J.; Evans, H. *J. Phys. Chem. Solids* **1971**, *32*, 2021.
(29) Creighton, J. A.; Deckman, H. W.; Newsam, J. M. *J. Phys. Chem.* **1994**, *98*, 448.

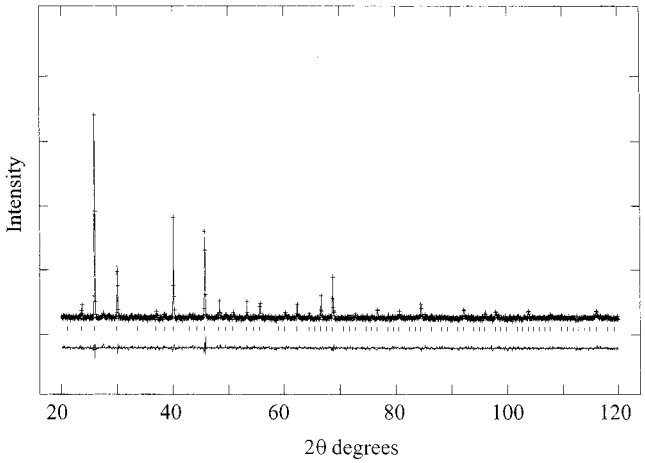

Figure 1. Rietveld refinement profile from X-ray diffraction data for $Mn_8[BeSiO_4]_6Te_2$. The upper broken line shows the experimental data and the continuous line the calculated pattern. The lower continuous line shows the fit.

analyzed and discussed in detail vibrational spectra from a variety of sodalite materials. Materials which crystallize with the sodalite structure in the space group $P\bar{4}3n$ should have 14 infrared-active framework absorption bands. Intensity calculations show that only nine of these vibrations have reasonable intensity. Typically, only six or seven of these can be readily resolved and these framework modes occur below 1200 cm^{-1}: three asymmetric stretches near 950 cm^{-1}, three symmetric bands in the region 700−1000 cm^{-1}, and one or two deformations at lower frequency, between 400 and 500 cm^{-1}. The frequencies of the symmetric stretches and the bend have been shown to be correlated with the sodalite lattice parameter and T−O−T bond angle in a number of sodalite systems showing a shift to lower frequency as the size of the cage increases. Figure 2a summarizes the positions and assignments of the seven characteristic absorption bands for the beryllosilicate sodalites:[17,31] three asymmetric (ν_{as}), three symmetric (ν_s), and one bend (δ). In Figure 2b only four absorption bands are correlated for the beryllogermanate sodalites[18,31] because the asymmetric bands are too close together to be discernible as three separate bands. In comparison to the case of the aluminosilicate sodalites, it is evident that although the number of infrared absorptions is maintained, the positions are shifted with the lower charged and smaller beryllium. For example, the symmetric stretches are in the range 690−765 cm^{-1} in comparison to those of the aluminosilicates, where the range is 630−740 cm^{-1}. From Figure 2 it can be seen that, for all the vibrations except one asymmetric stretch, a shift to lower frequency is observed as the size of the cage, and therefore the lattice parameter, increases; the frequency of the band at 950 cm^{-1} rises with increasing lattice parameter. The cause of this anomaly is due to the nature of this vibration where a change in bond angle accompanies this mode and increases the component of the oxygen displacement in the Be−Si direction. An effective increase in the compression of the T−O bond during the vibration results in an increase in energy of the mode and therefore a shift to higher wavenumbers.[30]

Structure. All the manganese beryllosilicate/germanate structures were successfully refined in the space group $P\bar{4}3n$, demonstrating an ordering of the beryllium and silicon (or germanium) atoms in the framework. The refined framework structure is depicted in Figure 3 and shows the coordination of the central Mn_4X unit. In all cases, the small Mn^{2+} ion (0.66 Å) coordinates tetrahedrally with three interactions with the close oxygens in the six-ring and one interaction with the central anion. The distance to the three distant oxygens in the six-ring are significantly over 3 Å and can be considered to be too long

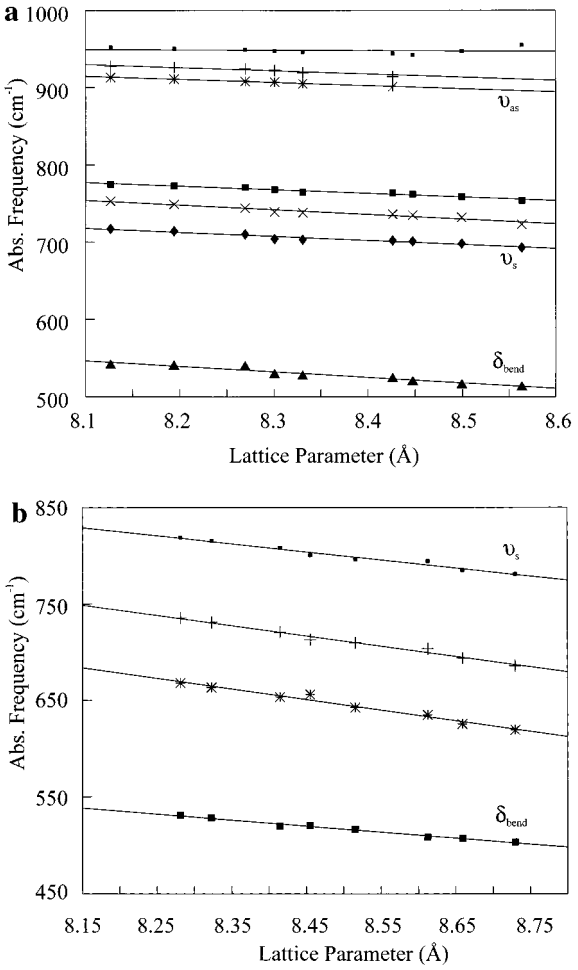

Figure 2. Correlation between the IR absorptions and the lattice parameter, with asymmetric vibrations in the range 900−1000 cm^{-1}, symmetric vibrations between 690 and 765 cm^{-1}, and a bend at 500 cm^{-1}: (a) the beryllosilicates; (b) the beryllogermanates.

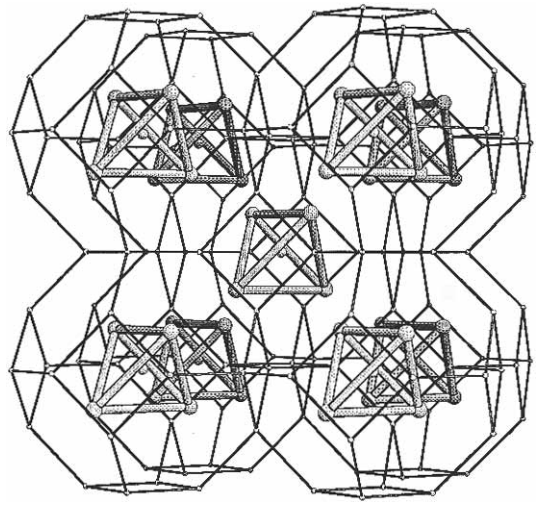

Figure 3. Part of the refined structure of $Mn_8[BeGeO_4]_6S_2$. The small gray spheres separated by the fine gray lines represent the framework At the center of each cage is a dark-gray tetrahedron representing the relationship of the four manganese cations (gray spheres).

(30) Brenchley, M. E.; Weller, M. T. *Chem. Mater.* **1993**, *5*, 970.
(31) Moran, K. L.; Harrison, W. T. A.; Gier, T. E.; Bu, X.; Herren, D.; Behrens, P.; Stucky, G. D. *Chem. Mater. Res.* **1996**, 1930.

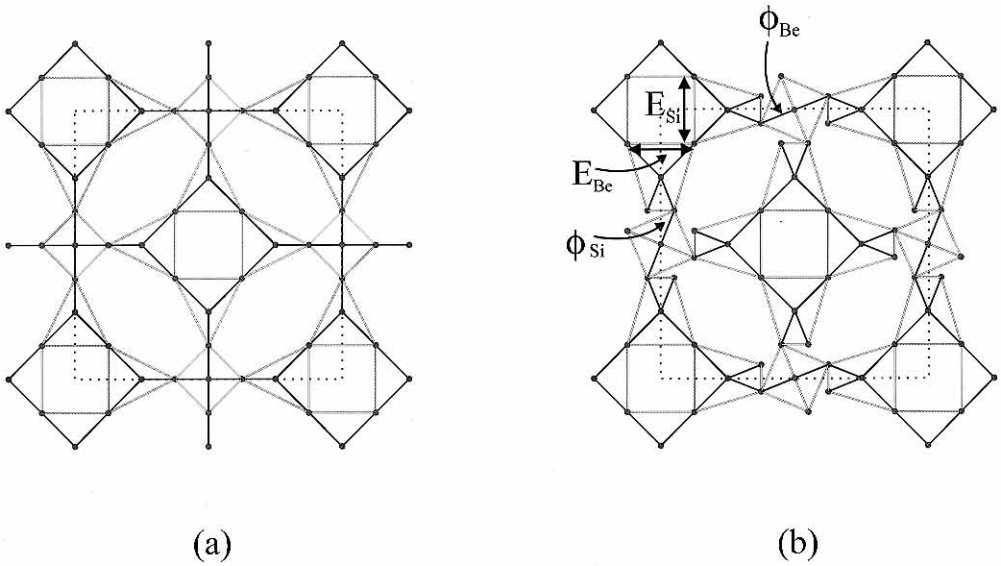

Figure 4. Upper half of the unit cell. (a) The fully expanded framework of regular tetrahedra of equal sizes (space group *Im*3*m*). Along each row of tetrahedra oriented with $\bar{4}$ axes parallel to a cell edge, alternate tetrahedra are rotated clockwise and anticlockwise. (b) The partially collapsed structure of sodalite showing rotation angles ϕ_{Be} and ϕ_{Si} and also O−O distances E_{Be} and E_{Si}.

for a typical Mn−O bond (ca 2−2.2 Å). The tetrahedral coordination around the central chalcogenide anion reflects closely that of the pure manganese chalcogenide with analogous Mn−X distances for Mn−S (beryllosilicate 2.453 Å, beryllogermanate 2.449 Å, and bulk 2.383 Å), Mn−Se (beryllosilicate 2.571 Å, beryllogermanate 2.562 Å, and bulk 2.549 Å), and Mn−Te (beryllosilicate 2.743 Å, bulk 2.725 Å). It should be noted that the refined oxygen parameters and temperature factors are slightly worse for refinements which used X-ray diffraction data rather than neutron diffraction data; oxygen has a small scattering factor compared with the other elements in the refinement (except beryllium which is on a fixed site) and would be expected to have larger esd's. The higher temperature factors result from the smaller usable data range in the X-ray diffraction experiment, where the sparse short *d*-spacing data provide little information on thermal disorder and thus worse temperature factors.

The sodalite structure can be understood by first considering a hypothetical fully-expanded framework of perfectly regular tetrahedra of equal sizes sharing corners (Figure 4). In actual sodalites, the framework collapses to allow reasonable coordination of the M cations to both the framework oxygens and the central anion. This is achieved by rotation of the tetrahedra about directions parallel to the cell edges and hence parallel to the improper 4-fold axes. The so-called partial collapse process may be characterized by an angle ϕ, known as the tilt angle, and as a result of the Be/Si alternation there are two values of ϕ, corresponding to the two different rotations of the Be- and Si-based centers in the framework. Computer modeling of the aluminosilicates by several workers has generated geometrical descriptions of the sodalite framework based on constant T−O distances; Taylor[32] established a computer model for the sodalite crystal structure which was later replaced by the distance least-squares modeling technique of Dempsey.[33] Hassan[34] proposed and developed a geometrical model for the sodalites and used this to calculate aluminosilicate framework geometries for a number of existing sodalites and predict values for theoretical materials. Although this assumption is simplistic, where small variations in the bond lengths are observed, this theory has led to satisfactory modeling for a wide range of sodalite materials. Using the crystallographic data obtained in recent structural work on the beryllosilicates/beryllogermanates[17,18,31] the geometrical model, as described in eqs 1 and 2, has been used to build

$$\cos\phi_{Si(Ge)} = \frac{1}{2E_{Si(Ge)}}\left[a - 4\left[(Be{-}O)^2 - \left(\frac{E_{Be}}{2}\right)^2\right]^{1/2}\right] \quad (1)$$

$$\cos\theta_{Be} = \frac{1}{2}E_{Be}\left[a - 4\left[(Si(Ge){-}O)^2 - \left(\frac{E_{Si}}{2}\right)^2\right]^{1/2}\right] \quad (2)$$

correlations between the tilt angle, ϕ, and the lattice parameter as shown in Figure 5, where E_{Si}, E_{Be} = 2.71 Å, E_{Ge} = 2.86 Å are the intratetrahedral O−O distances and Be−O, Si−O = 1.62 Å, Ge−O = 1.74 Å are the average bond lengths. Despite the simplicity of the model, the correlation of the beryllosilicate and beryllogermanate tilt angle with lattice parameter is very good, falling on an slightly curved path, as expected.[29]

UV/Vis Spectra. An example of the UV/vis spectra is shown for $Mn_8[BeSiO_4]_6Se_2$ in Figure 6, and the absorption bands and their assignments are tabulated in Table 3. The characteristic spectrum expected for a high-spin d^5 Mn^{2+} ion in a tetrahedral environment is observed in all cases; weak transitions are observed due to spin-forbidden transitions from the ^6S ground state to the spin quadruplet excited states. However, these are more intense for tetrahedrally coordinated ions than those normally found for a Mn^{2+} ion in a centrosymmetric octahedral environment. The four quartet states in the free ion split into ten component terms in the cubic crystal field, giving rise to ten possible transitions from the ground state. Generally only six (or seven) of these are resolvable. The transitions at 420 nm, i.e from ^6A to $^4E(G)$ and $^4A(G)$, are sharp because they are unaffected by either spin−orbit coupling (T states) or molecular vibrations as they are parallel to the ground state term, which allows easy assignment of the transitions in the UV/vis spectrum as given in Table 3.

Magnetic Behavior. The magnetic susceptibility of all the compounds followed the Curie−Weiss form $\chi = C/(T - \Theta)$ at temperatures between 50 K and room temperature; this is shown for $Mn_8[BeSiO_4]_6S_2$ in Figure 7, where $1/\chi$ is plotted versus *T*. The Curie−Weiss temperature, obtained by linear extrapolation to the negative temperature axis, is $\Theta = -124$ K, while the

(32) Taylor, D.; Henderson, C. M. B. *Phys. Chem. Miner.* **1978**, *2*, 325.
(33) Dempsey, M. J.; Taylor, D. *Phys. Chem. Miner.* **1980**, *6*, 197.
(34) Hassan, I.; Grundy, H. D. *Acta Crystallogr.* **1984**, *B40*, 6.

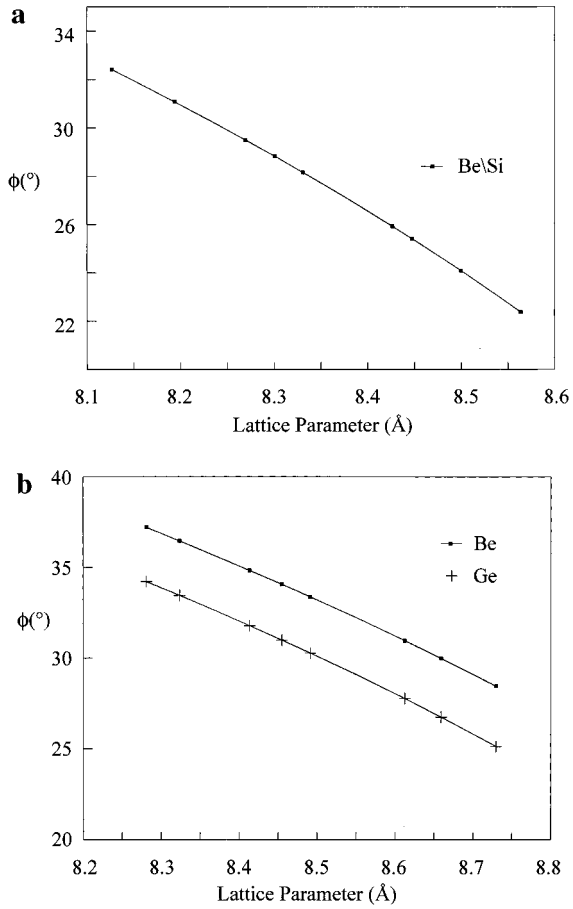

Figure 5. Correlation between tilt angles and lattice parameters for the (a) beryllosilicates and (b) beryllogermanates.

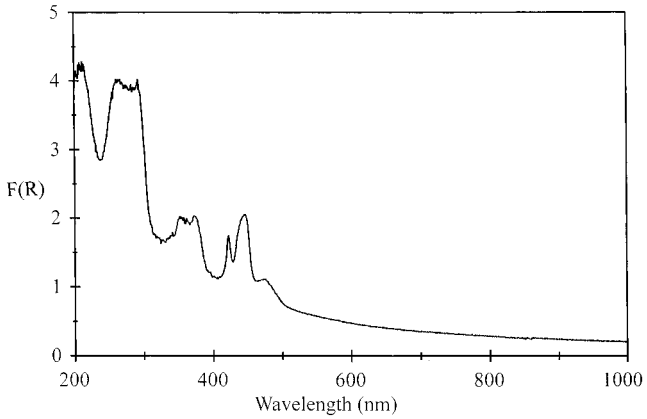

Figure 6. Diffuse reflectance UV/vis spectrum of $Mn_8[BeGeO_4]_6Se_2$ over the range 200−1000 nm showing characteristic spin-forbidden transitions for a tetrahedral d^5 cation.

Table 3. Assigments of UV/Vis Absorption Bands for $Mn_8[BeZO_4]_6X_2$ (nm)

Z/T	$^6A_1-$ $^4T_1(G)$	$^6A_1-$ $^4T_2(G)$	$^6A_1-^4E(G)$ $(^6A_1-^4A_1)(G)$	$^6A_1-$ $^4T_2(D)$	$^6A_1-$ $^4E(D)$
Z=Si, X=S	351	373	419	443	474
Z=Si, X=Se	353	375	420	444	476
Z=Si, X=Te	355	377	421	446	477
Z=Ge, X=S	353	375	420	441	472
Z=Ge, X=Se	358	378	422	449	478

Curie constant, C, corresponds to an effective paramagnetic moment $p_{eff} = 5.18\,\mu_B$. The large negative value of Θ indicates strongly antiferromagnetic exchange interactions between the magnetic ions, while the value of p_{eff} is a little smaller than the value expected for Mn^{2+} ions ($p_{eff} = g[S(S+1)]^{1/2} = 5.92\,\mu_B$ for $g = 2$ and $S = {}^5/_2$). Departures from Curie−Weiss behavior are apparent below 50 K, and a rounded maximum is found in the susceptiblity at 6 K (inset in Figure 7). The other compounds show similar behavior for $\chi(T)$, with $\Theta = -98.8$ K for $Mn_8[BeSiO_4]_6Se_2$ and $\Theta = -99.5$ K for $Mn_8[BeSiO_4]_6Te_2$. The maxima in the spectra for these two compounds occurred at 10.5 and 9.5 K, respectively.

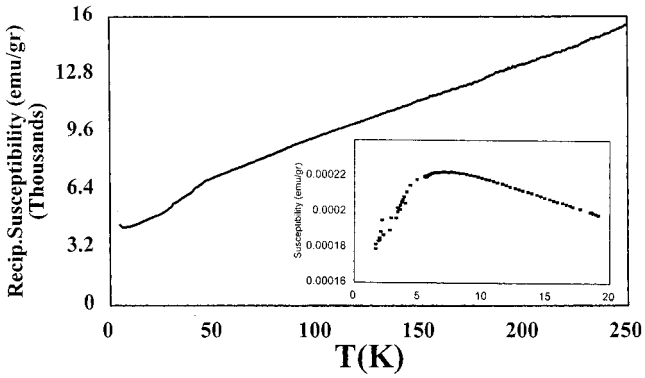

Figure 7. Reciprocal magnetic susceptibility curve for $Mn_8[BeSiO_4]_6S_2$ recorded over the temperature range 298−4.2 K showing loss in magnetization with temperature. Inset: low-temperature magnetic susceptibility curve.

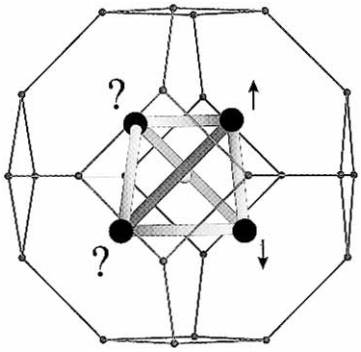

Figure 8. Magnetic frustration in a tetrahedral array of atoms.

Antiferromagnetic coupling between magnetic atoms which have tetrahedral coordination leads to geometrical frustration; any two of the four neighboring spins may be arranged antiparallel, but this does not allow the antiferromagnetic coupling of the remaining two spins to be satisfied (Figure 8). The ground state for a lattice of such tetrahedra possesses a high-spin degeneracy. Theoretical predictions for both classical Ising[35] and classical Heisenberg[36] spins suggest that no long-range magnetic order should exist in such lattices. Recent experimental work on pyrochlores,[37,38] such as $Tb_2Mo_2O_7$, which have corner-sharing tetrahedra, have shown strong antiferromagnetic exchange but only short magnetic correlation lengths, of the order of 5 Å, at low temperatures. The susceptibility behavior is spin-glass-like, with weak cusps and pronounced differences between field-cooled and zero-field-cooled data. It is very likely therefore that the rounded susceptibility maxima found for the present data correspond not to long-range antiferromagnetism but rather to spin-glass-like transitions, where the short-range magnetic order freezes in. Neutron scattering measurements are planned to study the magnetic correlations in detail.

(35) Anderson, P. W. *Phys. Rev.* **1956**, *102*, 1008.
(36) Villain, J. *Z. Phys. B* **1978**, *33*, 31.
(37) Greedan, J. E.; Reimers, J. N.; Stager, C. V.; Penny, S. L. *Phys. Rev. B* **1991**, *43*, 5682.
(38) Gaulin, B. D.; Reimers, J. N.; Mason, T. E.; Greedan, J. E.; Tun, Z. *Phys. Rev. Lett.* **1992**, *69*, 3244.

Experimental Section

The compounds were synthesized by solid state reactions in sealed quartz ampules at 1000−1100 °C. Mixtures of BeO, $Si(Ge)O_2$, MnO, and MnX (X = S, Se, Te) were homogeneously ground in an agate pestle and mortar in a glovebox (1 ppm of H_2O, 1 ppm of O_2) and placed in a quartz ampule. (MnX was previously made from the constituent elements in 1:1 molar ratio and reacted in sealed quartz ampules at 600 °C). The quartz ampule was sealed and placed inside a small alumina tube with glass wool at both ends to provide containment in the event of quartz tube failure. The alumina tube was then centered in a tube furnace and heated in stages to 400 °C for 4 h and then at 700 °C overnight. The tube was heated to the end point of 1000 °C (S, Se) or 1100 °C (Te) for a further 24 h. The tube furnace was then slow-cooled and the alumina tube removed once room temperature was attained. The product material was removed from the tube and washed with bromine water, adjusted to pH 6, to remove residual metal chalcogenide. The products ranged in color from pale yellow for the sulfides to green for the manganese beryllosilicate telluride.

Powder X-ray diffraction data were collected from the products using a Siemens D5000 diffractometer operating with Cu $K\alpha_1$ radiation. In all cases, the products were shown to be single-phase cubic materials which could be fully indexed in the space group $P\bar{4}3n$ except for the manganese telluride beryllogermanate sodalite. Unfortunately, no evidence of the manganese telluride beryllogermanate sodalite was ever seen, despite investigations at reaction temperatures of up to 1200 °C. The products were always Mn_2GeO_4, Be_2GeO_4, and MnTe. Presumably this is due to the stability of Mn_2GeO_4, which has been well characterized and has a structure related to olivine.[39] Refined cell parameters were as follows: beryllosilicates MnS 8.300(1) Å, MnSe 8.330(1) Å, MnTe 8.425(1) Å; and beryllogermanates MnS 8.455(1) Å, MnSe 8.515(1) Å. For structure refinement, powder X-ray diffraction data were collected over a 2θ range of 20−120° over a period of 15 h using a 0.02° step.

Powder neutron diffraction data were collected from single-phase products on the medium-resolution LAD instrument at the Rutherford Appleton Laboratories. Data were collected over the time-of-flight range 2000−19000 μs over a period of 6 h.

IR spectra were recorded from 4000 to 500 cm^{-1} using a Perkin-Elmer FT-IR 1710 equipped with a PE 3600 data station using pressed KBr disks. Diffuse reflectance optical absorption spectra were measured on undiluted samples using a Perkin-Elmer Lambda19 UV/vis spectrometer. The Kubelka−Munk correction was automatically applied to all spectra.

The magnetic behavior was recorded as a function of temperature on a vibrating-sample magnetometer (VSM) by cooling in a magnetic field of 0.05 T.

SEM and EDAX were performed using a JEOL JM2400 scanning microscope.

Acknowledgment. We thank the EPSRC for the funding of this work under Grant GR/H94900, Dr. Steve Hull for his help on the updated LAD instrument, and Dr. Barbara Cressey for her help with the EDAX analysis.

IC970511V

(39) Creer, T. *Solid State Commun.* **1970**, *9*, 1183.